Supernova light curves and spectra

Lecture notes for lessons 4-8 for "Stellar explosions", TUM, 2017

Anders Jerkstrand
anders@mpa-garching.mpg.de

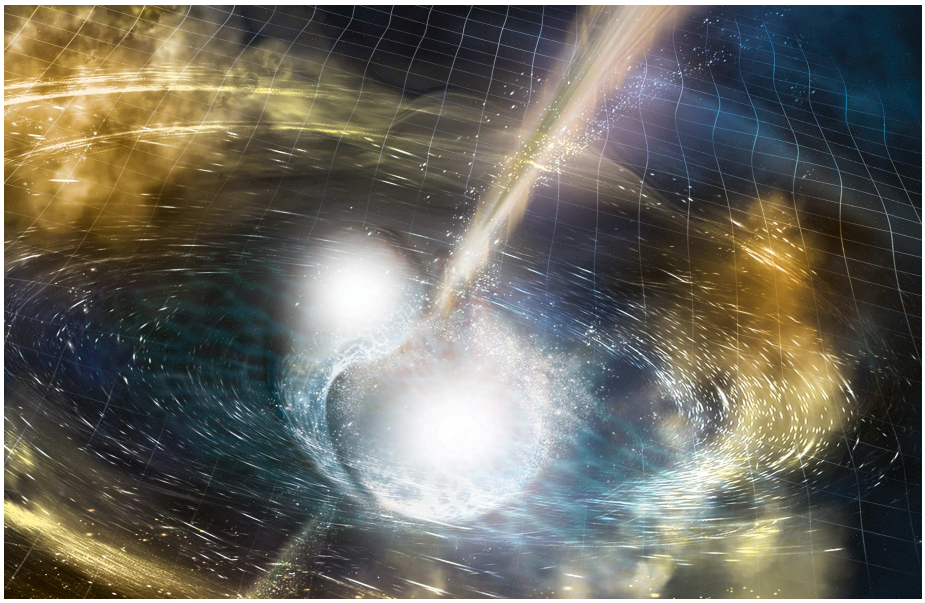

Overview

A CCSN explosion deposits an energy $E_{dep} \sim 10^{51}$ erg in the core of the star. This energy is spread to the whole star by a shock wave propagating with $v_{shock} \sim 10^4$ km s^{-1}. It reaches the surface after a time $t_{surf} = R_0/v_{shock}$, where R_0 is the stellar radius. We can estimate t_{surf} ∼1 minute for $R_0 = 1\ R_\odot$, t_{surf} ∼1 day for $R_0 = 500\ R_\odot$ (Red SuperGiant (RSG)). This begins the light display.

Equipartition. In the limit of **strong shocks** ($v_{shock} \gg v_{sound}$), one can show that radiation-dominated gas fulfills equipartition:

$$E^0_{int} = E^0_{kin} = \frac{1}{2} E_{dep} \tag{1}$$

I.e., in the shock wake, energy is equally divided between internal random energy and bulk kinetic energy (as the layers are both accelerated and heated). This limit is a good approximation for SNe ($v_{sound} \sim 10$ km s^{-1}).

Basic physics of the fireball

The first law of thermodynamics states that "the change in internal energy equals energy deposited, minus (net) energy transported out, minus work done (pdV)". For a moving gas we write this law on Lagrangian (comoving) form, where m is he coordinate rather than x or v:

$$\frac{\delta e_{int}(m,t)}{\delta t} = s(m,t) - \frac{\partial L(m,t)}{\partial m} - p(m,t)\frac{\partial\left(1/\rho(m,t)\right)}{\partial t} \tag{2}$$

Here e_{int} is the internal energy per unit mass (erg g^{-1}), s is the energy injection per unit mass and time (erg s^{-1} g^{-1}), L is the luminosity (erg s^{-1}), p is pressure (barye =dyne cm^{-2} = erg cm^{-3}), and ρ is the density (g cm^{-3}).

Energy density e_{int}. The internal energy consists of i) kinetic motions of particles ($3/2kT/\left(Am_p\right)$), where A is the atomic weight, ii) radiation field energy and iii) potential energy (excitation and ionization, $\sum_{i=1}^{Nions}\sum_{j=1}^{Nlevels}\epsilon_{i,j}$). In SNe radiation energy typically dominates. For a radiation field in thermal equilibrium:

$$e_{int} \approx e^{rad}_{int} = aT^4/\rho \tag{3}$$

where a is the radiation constant $a = 7.56 \times 10^{-15}$ erg cm^{-3} K^{-4}.

Pressure p. The pressure can be expressed in terms of T and ρ by an equation of state, which for radiation-dominated gas depends only on T and is

$$p = \frac{1}{3}aT^4 = \frac{1}{3}e_{int}\rho \tag{4}$$

Homologous expansion. Quite soon the material reaches ballistic trajectories (velocity V constant). After some further time, $R \approx Vt$ holds, so called

homology. Then $\rho(t) \propto M/R(t)^3 \propto t^{-3}$ and

$$\frac{\partial 1/\rho}{\partial t} = \frac{-3}{\rho t} \tag{5}$$

We will return later to the term for radiation transport. If we assume both this term and $s(m,t)$ are unimportant, we get the adiabatic limit:

$$\frac{\delta e_{int}(m,t)}{\delta t} = -\frac{e_{int}(m,t)}{t} \tag{6}$$

which has solution $\boxed{e_{int} = e_{int,0}\,(t/t_0)^{-1}}$ or $T^4/t^{-3} \propto t^{-1} \rightarrow \boxed{T \propto t^{-1}}$.

Diffusion and light curve duration

Let λ be the mean-free-path, the typical length photons travel before interacting with matter. We have $\lambda = 1/(\kappa\rho)$, where κ is the opacity ($\mathrm{cm}^2\ \mathrm{g}^{-1}$). The time between interactions is then λ/c. If N is the required number of scatterings to escape the nebula, the total diffusion time is $t_{diff} = N\lambda/c$. One can show that $N \approx \tau^2$ where $\tau = R/\lambda$ is the optical depth. Then

$$t_{diff}(t) = \frac{R(t)^2\kappa(t)\rho(t)}{c} \tag{7}$$

Using homology ($R(t) = Vt$) and $\rho \approx M/(4\pi/3R^3)$, we get

$$t_{diff}(t) = \frac{3}{4\pi}\frac{\kappa(t)M}{Vtc} \tag{8}$$

Using $E = 1/2MV^2$, and finally equating $t_{diff}(\Delta t) = \Delta t$, where Δt is the typical duration of the light curve, we get

$$\boxed{\Delta t = 30d\ E_{51}^{-1/4} M_{M_\odot}^{3/4} \kappa_{0.4}^{1/2}} \tag{9}$$

where $E_{51} = E/10^{51}$ erg, $M_{M_\odot} = M/1\ M_\odot$, and $\kappa_{0.4} = \kappa/0.4\ \mathrm{cm}^2\mathrm{g}^{-1}$.

That the SN diffuses as long as $t \lesssim t_{diff}$ (so $t_{diff}(\Delta t) = \Delta t$) can be shown from numeric simulations, but also also qualitatively understood. If $t_{diff} \ll t$ the diffusion phase is already over and the LC is declining. If $t_{diff} \gg t$ the radiation will take much longer than t to get out and the LC is still rising. The peak occurs roughly when these time-scales match. Although a simplistic derivation, the *scalings* (the exponents) are quite accurate compared to actual numerical simulations. The weak sensitivity to E means that one can estimate $M\kappa^{2/3}$ quite accurately from the duration of the LC (uncertainty in E has minor impact).

Type IIP SNe : considering recombination

The behaviour of Type IIP SNe is somewhat more complex due to rapid time and space-dependent changes in opacity. When the temperature in a layer reaches the H recombination temperature ($T_{rec} \sim 6000$ K), the opacity drops to almost zero and energy in that shell is released. A better approximative approach is to combine $L = 4\pi R^2 \sigma T_{rec}^4$ and $L = E_{int}(t = \Delta t_{IIP}/2)/\Delta t_{IIP} = (ER_0/V\Delta t_{IIP})/\Delta t_{IIP}$ (we deployed here the adiabatic limit), to get

$$\boxed{\Delta t_{IIP} = 40d\ E_{51}^{-1/8} R_{0,500}^{1/4} M_{M_\odot}^{3/8}} \tag{10}$$

Here $\sigma = 5.67 \times 10^{-8}$ erg cm^{-2} s^{-1} K^{-4} is the Stefan-Boltzmann constant and $R_{0,500} = R_0/500R_\odot$. In this framework

- The dependency on E and M is weaker than in Eq 9. This weakness means the LC duration (alone) does not constrain these parameters to high accuracy.
- R_0 replaces κ as a parameter. But weak dependency also for R_0.

We know that RSGs have $R_0 \sim 500\ R_\odot$. If we assume $E_{51} = 1$, their typical duration of 120d tells us $M \sim (120/40)^{8/3} \sim 18\ M_\odot$.

These analytic considerations are not only useful for simple fitting procedures. They fundamentally tell us about sensitivities and what is likely to be obtained from carrying out more detailed simulations. For example, it is clear that E and R_0 cannot readily be extracted from a IIP LC length, no matter how detailed model. The weak scaling also give us a first explanation for the relatively homogeneity of IIP light curves; they all have rather similar length (120d). As different progenitors would still have R_0, E and M similar to factor few, the variety in Δt_{IIP} is quite small.

Brightness

a) Explosive energy release

One can show that with only explosive energy, the LC reaches bolometric peak almost immediately, and then declines. The typical brightness can be estimated as the internal energy at time Δt divided by the diffusion time $t_{diff} \approx \Delta t$. Using again the adiabatic limit:

$$L \approx \frac{E/2(R(t = \Delta t)/R_0)^{-1}}{\Delta t} = \frac{E/2R_0}{V\Delta t^2} = \frac{E/2R_0}{2^{1/2}E^{1/2}M^{-1/2}\Delta t^2} \tag{11}$$

Insert now $\Delta t = 30d\ E_{51}^{-1/4} M_{M_\odot}^{3/4} \kappa_{0.4}^{1/2}$ from above. Then

$$\boxed{L = 3 \times 10^{42} E_{51} M_{M_\odot}^{-1} R_{0,500} \kappa_{0.4}^{-1}\ \text{erg s}^{-1}} \tag{12}$$

We make the following observations

- **Brightness increases (linearly) with** E. This is not as simple as "put twice as much in and twice as much comes out". Higher E leads to a larger energy reservoar (E^1 factor), but also to higher velocities, which gives stronger adiabatic degradation to a given radius ($E^{1/4}$ factor). But this is offset by a shorter diffusion time ($E^{-1/4}$ factor), so these two effects cancel and leave only the first one.

- **Brightness increases (linearly) with** R_0. This is because larger R_0 means less adiabatic cooling can occur for a given time. Compact stars like Wolf-Rayet and He cores have $R_0 \sim 1\ R_\odot$. Then, without further energy input they peak at about 10^{40} erg s^{-1}. Explosion of whife dwarfs ($R_0 \sim 0.01 R_\odot$) would peak at 10^{38} erg s^{-1}.

- **Brightness decreases (linearly) with** M. Increasing M leads to lower velocities, higher densities, and more trapping of the radiation. Radiation then gets spread out over a longer diffusion time ($M^{3/4}$ factor), and also degrades more adiabatically ($M^{1/4}$ factor).

- **Brightess decreases (linearly) with** κ. Spreading the energy release over a longer diffusion time both dilutes by the time itself ($\kappa^{1/2}$ factor) and leads to more adiabatic degradation over this longer time ($\kappa^{1/2}$ factor).

However, it turns out that only Type II SNe, which come from RSGs, have light curves governed by release of energy deposited in the explosion. Type I SNe come from compact stars (white dwarfs, Wolf-Rayet stars, He stars), but are still as bright as Type II SNe. The explanation for this is that SNe also have another energy source; radioactivity.

Type IIP SNe

With the alternative derivation for Type IIP SNe, one gets

$$L \propto E^{3/4} M^{-1/4} R_0^{1/2} T_{rec}^2 \tag{13}$$

All scalings here are weaker than in Eq 12. Considering both equations, the brightness is mainly a potential diagnostic of E, but also this dependency is sublinear. Fig. 1 shows a collage of observed IIP light curves.

b) Radioactivity

Table 1 shows the peak brightness of different transients predicted by Eq. 12 and observed ones. It is clear that, apart from Type IIP SNe, the theory of shock deposited energy leakage is not the right explanation for SN brightness. Instead, the energy release for Type Ibc, Ia and KNe is dominated by radioactivity. The most important isotope for SNe is ^{56}Ni, which decays to ^{56}Co on a time-scale of 8d, and then to ^{56}Fe on a time-scale of 111d. A total ^{56}Ni mass of $\sim 0.1\ M_\odot$

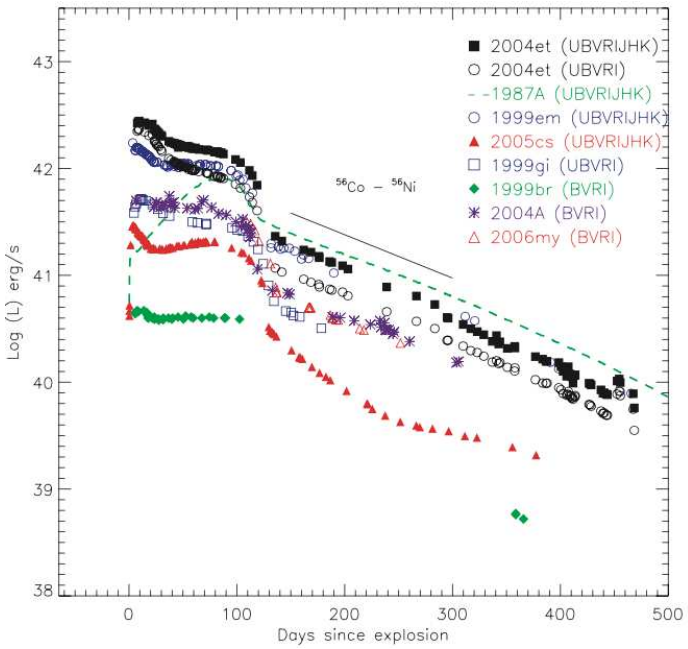

Figure 1: A collection of Type IIP bolometric light curves. Can you explain why plateau durations are similar, but brightness vary a lot, both during plateau and in the nebular tail phase? Why does brighter plateau associate with brighter tail phase? From Maguire et al. 2010.

is made in CCSNe and $\sim$0.5 $M_\odot$ in TNSNe. Q-value = 5.5 MeV/decay $\rightarrow$ total energy decay is

$$E_{decay} \approx \frac{M(^{56}\mathrm{Ni})}{56 m_p} \times 5.5 \times 10^6 \text{ eV} \approx 2 \times 10^{49} \left(\frac{M(^{56}\mathrm{Ni})}{0.1\ M_\odot} \right) \text{ erg} \qquad (14)$$

where 1 eV $= 1.6 \times 10^{-12}$ erg. This is over 20 times smaller than the explosive energy, but released on long time-scale which avoids much adiabatic degradation (factor $\sim 10^4$ for $R_0 = 1\ R_\odot$ and $t = 10d$).

Star	SN type	R_0 ($R_\odot$)	L_{peak} (Explosive, Eq 12) (erg/s)	L_{peak} (Observed) (erg/s)
RSG	IIP	500	3×10^{41} ($M_{M_\odot} = 10$)	$3 \times 10^{40} - 3 \times 10^{42}$
BSG	II-pec	50	3×10^{40} ($M_{M_\odot} = 10$)	$\sim 1 \times 10^{42}$
WR star	Ibc	5	3×10^{40} ($M_{M_\odot} = 10$)	$\sim 1 \times 10^{42}$
WD	Ia	0.01	6×10^{37} ($M_{M_\odot} = 1$)	$\sim 1 \times 10^{43}$
NS	KN	10^{-4}	6×10^{37} ($M_{M_\odot} = 0.01$)	$\sim 1 \times 10^{42}$

Table 1: Peak luminosities of different SN classes.

One can show that to within factor 2 or so, radioactive powered LCs obey "Arnett's law"

$$\boxed{L_{peak} \approx S(t_{peak})} \tag{15}$$

where S denotes the total energy injection rate ($\int sdm$). This is useful to estimate the ^{56}Ni mass in SNe. For example, ^{56}Co decay obeys roughly

$$S = 1.4 \times 10^{42} \left(\frac{M(^{56}\mathrm{Co})}{0.1\ M_\odot} \right) \exp\left(-t/111d\right) \mathrm{erg/s} \tag{16}$$

Exercise: The brightest supernovae peak at $L \sim 10^{44}$ erg/s after about 30d. Can they be radioactively powered?
Solution: Arnett's law: M(^{56}Ni) = 10 $M_\odot$. But $\Delta t = 30d \rightarrow E_{51}^{-1/4} M_{M_\odot}^{3/4} \kappa_{0.4}^{1/2} = 1 \rightarrow M = 1\ M_\odot E_{51}^{1/3} \kappa_{0.4}^{-2/3}$. Unless E and κ are unphysically large/low, $M(^{56}\mathrm{Ni}) > M$, which of course is impossible. In addition, the spectra show mostly O, Mg, and Ca, not Fe. Therefore, it has been proposed that the powering comes from something else (more later).

Surface temperature and spectral shape

Define the photosphere R_{phot} as the radius from which photons can escape freely ($\tau \approx 1$). Assume for now this is wavelength independent. Assuming blackbody emission, we have

$$L(t) = 4\pi R_{phot}(t)^2 \sigma T_{phot}(t)^4 \tag{17}$$

Writing $R_{phot}(t) = V_{phot}(t)t$:

$$T_{phot}(t) = \left(\frac{L(t)}{4\pi\sigma V_{phot}(t)^2} \right)^{1/4} t^{-1/2} \tag{18}$$

For order of magnitude, take typical $L_{peak} = 10^{42}$ erg/s, $t_{peak} = 30d$ and $V_{phot} = 5000$ km/s, $\rightarrow T_{phot} = 5300$ K. SNe peak at "optical temperatures" ($T_{\rm sun} = 5800K$).

For the radioactivity peak:

- During pre-peak: L is increasing (and V_{phot} is decreasing) so T_{phot} evolves *slower* than $t^{-1/2}$, and can even increase.
- Around peak: L is roughly constant, V_{phot} is slowly decreasing, so T_{phot} follows $t^{-1/2}$ or somewhat slower. This means that *redder bands peak later*.
- During post-peak: L is decreasing rapidly, while V_{phot} evolves slowly, and evolution is typically faster than $t^{-1/2}$.

  Figure 2 shows an observed evolution in these three phases. Typically, observations of L and T_{phot} are used to determine the $R_{phot}(t)$ evolution, which constrains models. At about twice the peak time, the diffusion is over and the SN enters the nebular phase. The assumption of a photosphere emitting a blackbody then breaks down.

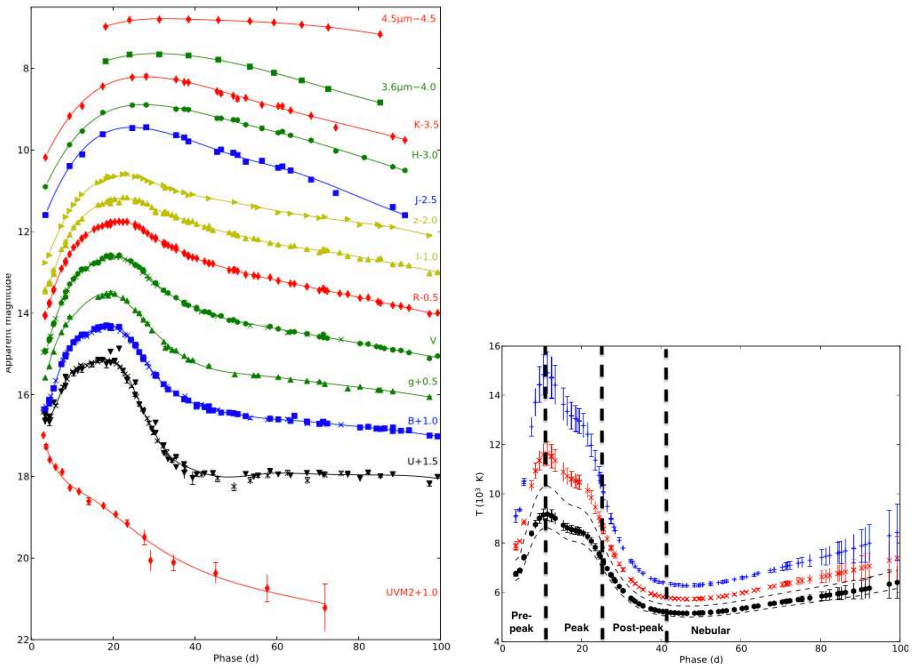

Figure 2: Evolution of light curve in different photometric bands (left) for a radioactivity-powered Type IIb SN and (right) T_{phot} evolution (black dots, ignore other plotted quantities). From Ergon et al. 2014.

Application: AT2017gfo - the first kilonova

August 17 2017: First gravitational wave detection of two merging neutron stars at 40 Mpc. A SN-like transient, called **kilonova** (KN), followed (see Fig. 3). It had the following properties:

$$t_{peak} = 1 \text{ day} \tag{19}$$

$$L_{peak} = 10^{42} \text{ erg s}^{-1} \tag{20}$$

$$T_{phot} \sim 8500 \text{ K}. \tag{21}$$

Exercise: Estimate M, E, κ from these three observables. Also need to know $s = 4 \times 10^{43} M_{M_\odot} t_{days}^{-1.2}$ erg/s for KNe.
Solution:

A. From Arnett's rule, $M_{M_\odot} = 10^{42}/(4 \times 10^{43} \times 1^{-1.2}) = 0.025$.

B. From LC duration:

$$E_{51}^{-1/4} M_{M_\odot}^{3/4} \kappa_{0.4}^{1/2} = \frac{1}{30} \tag{22}$$

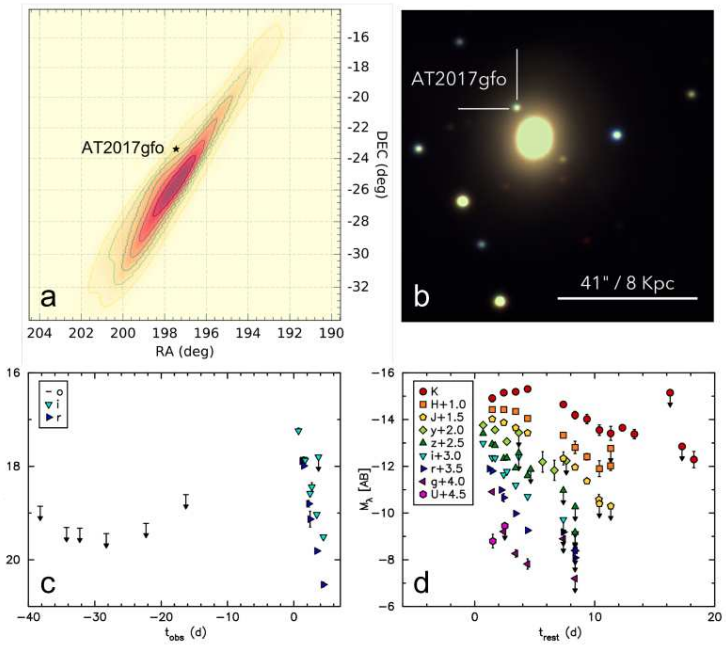

Figure 3: The first kilonova. *Top left*: location of the transient compared to the region indicated by the gravitational wave detection. *Top right*: Image of the KN and its host galaxy. *Bottom right*: Photometric evolution in different bands; successively longer wavelengths from U to K. From Smartt et al. 2017.

C. From blackbody equation

$$V_{phot}(t = t_{peak}) = \left(\frac{L_{peak}}{4\pi t_{peak}^2 \sigma T_{phot}^4} \right)^{1/2} = 6 \times 10^9 \text{ cm s}^{-1} = 0.2c \quad (23)$$

D. Now, approximate $E = 1/2 M V_{phot}^2$. Then

$$E_{51} = 1/2 \times 0.025 \times 2 \times 10^{33} \times \left(6 \times 10^9\right)^2 / 1 \times 10^{51} = 0.9 \quad (24)$$

Finally, plug back into step 2:

$$\kappa_{0.4} = \left(\frac{1}{30} \times 0.9^{1/4} \times 0.025^{-3/4} \right)^2 = 0.27 \quad (25)$$

So $\kappa = 0.4 \times 0.27 = 0.11$ cm^2 g^{-1}.

Kilonovae have one fundamental difference to SNe: the power term is directly related to $M_{M_\odot}$ because *all* the ejecta is radioactive. In SNe only ^{56}Ni is radioactive. This means that we have <u>five</u> unknowns $(M, M_{56Ni}, E, V, \kappa)$, but

still only 4 equations (1-4 above). The typical solution is to assume a value for κ (or calculate it given a composition).

There is a possible fifth equation to use: consideration of escape of gamma rays from the ejecta (which becomes optically thin to Compton scattering after a few months). But it requires late-time data, and in principle introduces also yet another parameter: the mixing (location) of ^{56}Ni in the ejecta.

Another difficulty is what velocity to use for proxy to $V = \sqrt{2E/M}$. V_{phot} can be quite different and is not very accurate in general, but there are no other options, unless one wants to compute more advanced models.

Exercise: Assume that κ is well known, but there is a factor 2 error in estimating V. What error does this lead to in M? In E?
Solution: Cancelling M in the equations above, one obtains $E \propto \Delta t^2 V^3 \kappa^{-1}$. A factor 2 error in V thus gives a factor 8 wrong E. Instead cancelling E, one obtains $M \propto \Delta t^2 V \kappa^{-1}$, thus mass obtains a factor 2 error.

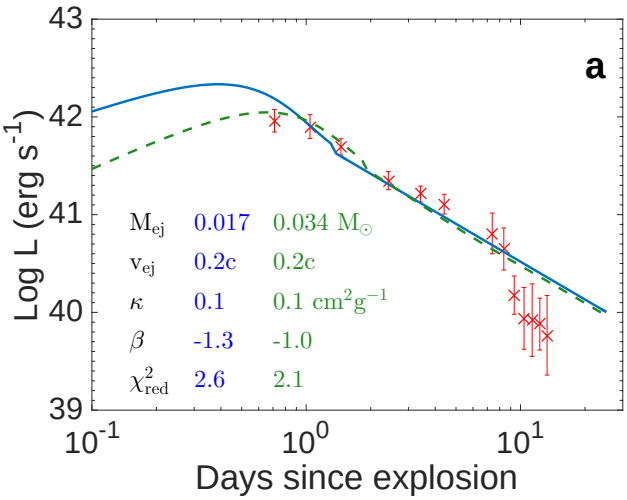

Figure 4: Observed bolometric light curve of the first kilonova, and two simple models. These models use semi-analytic expressions (the luminosity at time t is an integral of the energy input at all ealier times, weighted by a kernel that depends on ejecta properties. Such formulas can be derived from basic equations such as Eq. 2 plus certain simplifying assumptions. From Smartt, Chen, Jerkstrand et al, Nature 2017.

Radiation-matter interactions

The interaction of photons and matter is dominated by photon-electron interactions. The electron can be free, or bound in an atom (or molecule or dust grain). We will consider four main processes.

1) Electron scattering

In the frame of the electron, for $E_{photon} \ll m_e c^2(511 \text{ keV})$, photons scatter, i.e. change direction but not energy. This is called Thomson scattering. Often the most important source of interaction. The cross section is wavelength-independent ("gray") : $\sigma_{es} = 6.7 \times 10^{-25}$ cm^2. Then

$$\kappa^{es} = \frac{n_e \sigma_{es}}{\rho} = \frac{n_{nucleons} Y_e x_e}{n_{nucleons} m_p} = 0.4 Y_e x_e \text{ cm}^2\text{g}^{-1} \tag{26}$$

where $Y_e = n_e/(n_{nucleons})$ is the electron fraction, x_e is the ionization degree (0-1). Examples:

- Pure H, fully ionized : $Y_e = 1$, $x_e = 1$, $\rightarrow \kappa^{es} = 0.4$ cm^{2}g^{-1}.
- Pure He, singly ionized: $Y_e = 0.5$, $x_e = 0.5$, $\rightarrow \kappa^{es} = 0.1$ cm^{2}g^{-1}.

All elements except H have $Y_e \approx 0.5$. If half ionized, $\kappa^{es} = 0.1$. Often used approximation when little else known.

At $E_\gamma \gtrsim m_e c^2$, the recoil energy of the electron becomes a significant fraction of the photon energy: the scattering becomes incoherent as the photon always loses a significant fraction of its energy. In this limit (called Compton scattering), the cross section is also smaller, declining with energy. At 1 MeV is is $1/3\sigma_T$.

How long is a spherical SN of mass M and kinetic energy E, optically thick to electron scattering?

$$\tau_{es} = \kappa^{es} \rho R = \kappa^{es} \frac{M}{4\pi/3 R^2} = \kappa^{es} \frac{M}{4\pi/3 V^2 t^2} = \kappa^{es} \frac{M^2}{8\pi/3 E t^2} \tag{27}$$

Putting $\tau_{es} = 1$ we get

$$\boxed{t_{thick} = 160\text{d } (\kappa^{es}_{0.4})^{1/2} M_{M_\odot} E_{51}^{-1/2}} \tag{28}$$

But Type IIP SNe have $M_{M_\odot} \approx 10$ and then we get $t_{thick} = 1600d$. We know that they become optically thin to electron scattering much earlier, around 200d. The reason for the discrepancy is that they continously recombine (so $\kappa^{es}_{0.4} \sim 1$ is not accurate). By 200d, $x_e \sim 0.01$, which brings $\kappa_{0.4}$ down to 0.01, and t_{thick} down to 200d.

What about Ia SNe? They are ~ 1 $M_\odot$ ejecta of mostly iron. Spectra tell us ejecta are roughly doubly ionized, so $x_e \sim 2/26 = 0.08$, so $\kappa^{es} = 0.016$, and $(\kappa^{es}_{0.4})^{1/2} = 0.2$, giving $t_{thick} \approx 30$d. Similar parameters hold for Ibc SNe, so we conclude these diffuse for a few weeks.

2) Free-free absorption

A photon can be absorbed by an electron in the presence of a third positively charged body such as a proton or a He+ ion. Averaged of a thermal distribution of electrons:

$$\boxed{\kappa_\lambda^{ff} = 0.8 T_4^{-1/2} \lambda_{\mu m}^3 \left(1 - e^{-hc/\lambda kT}\right) \left(\frac{n_e}{10^{13}\ \mathrm{cm}^{-3}}\right) Z^2 \bar{A}^{-1}}\ \mathrm{cm}^2\mathrm{g}^{-1} \quad (29)$$

Here Z is the charge of the ion and $\bar{A}$ its atomic number. Two important properties are

- For a blackbody field the bulk of radiation has $hc/\lambda \geq kT$, so $1 - \exp(-hc/\lambda kT)$ is close to unity.
- While κ^{es} is independent on n_e, κ^{ff} is proportional to it (due to its 3-body nature). It then evolves more rapidly in time.

The electron density follows (uniform sphere case)

$$n_e = 4.4 \times 10^{14} M_{M_\odot}^{1/2} E_{51}^{-1/2} t_d^{-3} x_e(t)\ \mathrm{cm}^{-3} \quad (30)$$

Thus, for this opacity to be relevant compared to κ^{es} in the optical/UV

$$\boxed{t \lesssim (4 \times 10^{14}/1 \times 10^{13})^{1/3} \sim 4d} \quad (31)$$

In practice, free-free absorption plays only a secondary role for opacity for the following reason; the density needs to be high for κ^{ff} to be large, but at high density, the temperature is also high, and λ^3 is then small. Thus, in no regime are both of these factors favorable. Free-free opacity plays however a large role to interpret IR observations. For example, at $\lambda \gtrsim 10\mu$m the SN can remain optically thick for many months.

3) Photoionization

A photon can eject a bound electron in a photoionization, if $E_{photon} > E_{binding}$. This is also called bound-free absorption. For hydrogen and hydrogenic ions

$$\sigma_\lambda^{pi} \approx 10^{-17} \left(\frac{\lambda}{\lambda_0}\right)^3\ \mathrm{cm}^2 \quad (32)$$

where λ_0 is the ionization threshold ($= hc/E_{binding}$), which is 912 Å for the ground state of hydrogen. Then (for H)

$$\kappa_\lambda^{pi} = \frac{\sigma_\lambda^{pi}(1 - x_e)}{m_p} = 6 \times 10^6 (1 - x_e) \left(\frac{\lambda}{\lambda_0}\right)^3\ \mathrm{cm}^2\mathrm{g}^{-1} \quad (33)$$

Clearly, as long as even a minor amount of H is neutral ($1 - x_e \gtrsim 10^{-7}$), $\kappa^{pi} \gg \kappa^{es}, \kappa^{ff}$ at wavelengths close to threshold. Some other element thresholds:
If the radiation field peaks in the hard UV (100-1500 Å), p.i. can be expected to be important. From Wien's displacement law, $\lambda_{peak} = 0.29/T$ cm, giving $20,000 < T < 300,000$ for this condition.

Element	λ_0
He I	504 Å
O I	912 Å
O II	353 Å
Fe I	1568 Å
Fe II	766 Å
Fe III	404 Å

Table 2: Photoionization ground state threshholds for some common atoms and ions.

At later times, $1 - x_e \to 1$ and one might expect κ^{pi} to gain in importance. However, then $T \ll 20,000$ K $\to$ few photons have enough energy. As for free-free absorption, two conditions are required which are not easily met at the same time in SNe.

Excited states. The thresholds λ_0 move to longer wavelengths for p.i. from excited states, e.g. n=2 in HI has a threshold at 3646 Å. A significant fraction of photons have such energies for $T \gtrsim 5000$ K. However, the number of atoms in these excited states is typically much smaller than in the ground state.

4) Line absorption

A photon can be absorbed and cause a photoexcitation of a bound electron from a lower state l to an upper state u. This is also called a bound-bound transition. The cross section can be written

$$\sigma_\lambda^{bb} = \Phi_0 \phi(\lambda - \lambda_0) \tag{34}$$

where ϕ is the line profile (unit cm^{-1}), which is normalized so $\int \phi d\lambda = 1$. The strength of the line is given by the parameter

$$\Phi_0 = \frac{h\lambda_0}{4\pi} B \tag{35}$$

where B is the Einstein absorption coefficient (unit cm^2 ster erg^{-1} s^{-1}), which can be of order 10^{10} for strong lines, giving $\Phi_0 \sim 10^{-22}$ cm^3 in the optical. Thermal broadening is of order $V_{th} = \sqrt{kT/m_p} \sim 1$ km s^{-1}, or $\Delta\lambda_{th} = \lambda_0 V_{th}/c \sim 10^{-10}$ cm, so $\sigma \sim 10^{-12}$ cm^2 for a strong line if we take $\phi \sim 1/\Delta\lambda$. Then, for a box-like profile

$$\kappa_{\lambda 0}^{bb} = \frac{\sigma^{bb}}{m_p} = \frac{h\lambda_0}{4\pi} B \frac{1}{\Delta\lambda_{th} m_p} \sim 10^{12} \text{ cm}^2\text{g}^{-1} \tag{36}$$

A line can provide huge opacity over its profile, 10^{12} times electron scattering, but if the photon field covers say 10^4 Å, only a fraction 10^{-6} would interact with the line. It is clear that to understand line opacity, we must obtain information on the total number of lines, and have to consider radiation field with

wavelength dependence. We also have to think about how the Doppler shifts between different parts of the SN enter the problem (more later).

The excited atom typically relaxes back by spontaneous photon emission (rate A s^{-1}, where A is the Einstein emission coefficient), either in the same transition ("resonance scattering") or in a set of branching ones ("fluorescence"). It can also be collisionally deexcited by a free electron ("thermalization"), but the chance of this is typically lower.

What happens to the energy?

Consider now Table 2, summarizing what happens to the radiative energy following an interaction. In many situations electron scattering and line absorption are the dominant processes. But neither of these couple strongly to the thermal energy in the electrons and atoms in the gas. Free-free and bound-free absorption play an important tole in providing this coupling, which resets the distribution and brings conditions close to "local equilibrium".

Process	Scattering/Fluorescence	Thermalization	Potential energy
Thomson	100%	0%	0%
Free-free	0%	100%	0%
Bound-free	0%	Part	Part
Line	Mostly	Minor	0%

Table 3: A summary of the fate of the radiative energy following an interaction.

Radiative transfer

We need to consider how radiation propagates in the SN, e.g. for the dL/dm term in the 1st law of TD, and to obtain the emergent spectra. For this we use radiative transfer theory.

Quantities

The radiative energy travelling per unit area, per unit time, per unit Hz, per unit solid angle, is the specific intensity. In spherical symmetry it depends on 4 variables:

$$I_\nu(r,\theta,t) \quad (\text{erg s}^{-1}\text{cm}^{-2}\text{Hz}^{-1}\text{Ster}^{-1}) \tag{37}$$

wher θ is the angle relative to the radial direction. This quantity is related to the monochromatic photon number density

$$\phi_\nu = \frac{1}{ch\nu} I_\nu \quad (\text{cm}^{-3}\text{Hz}^{-1}) \tag{38}$$

The mean intensity is the angle-average of I_ν:

$$J_\nu = \frac{1}{4\pi}\int I_\nu d\Omega \qquad (\text{erg s}^{-1}\text{cm}^{-2}\text{Hz}^{-1}\text{Ster}^{-1}) \tag{39}$$

where $\int \Omega = \int_{\theta=0}^{\pi}\int_{\phi=0}^{2\pi}\sin(\theta)d\theta d\phi$, so $J_\nu = \frac{1}{2}\int I_\nu \sin(\theta)d\theta$. This is related to the monochromatic energy density

$$E_\nu = \frac{4\pi}{c} J_\nu \quad (\text{erg cm}^{-3}\text{Hz}^{-1}) \tag{40}$$

The radiation flux (or first moment) is

$$F_\nu = 2\pi \int I_\nu \cos\theta \sin\theta d\theta \quad (\text{erg s}^{-1}\text{cm}^{-2}\text{Hz}^{-1}) \tag{41}$$

The momentum of a photon is $p = h\nu/c$. The momentum flow is then $p\phi_\nu c = h\nu/(c^2 h\nu) I_\nu c = I_\nu/c$. If there is an angle between the flow direction and surface, a $\cos^2$ term enters (one for component of the momentum, one for area projection). Then, the specific pressure (second moment) is

$$p_\nu = 2\pi \int \frac{I_\nu}{c} \cos^2(\theta)\sin(\theta)d\theta \tag{42}$$

If the radiation field is isotropic, $I_\nu = J_\nu$ and

$$p_\nu = \frac{2\pi J_\nu}{c}\left[\frac{\mu^3}{3}\right]_{-1}^{1} = \frac{4\pi J_\nu}{3c} = \frac{1}{3}E_\nu \tag{43}$$

When integrating over frequency, this is the derivation of $p = 1/3aT^4$ used earlier (Eq. 4).

Transfer equation

The transfer equation is the "bookkeeping equation" for radiation field energy. Its generic form is

$$\frac{dI_\nu}{ds} = \eta_\nu - \chi_\nu I_\nu \tag{44}$$

with interpretation "change in I_ν equals addition into the beam minus absorption out of the beam". Here η_ν is the emission coefficient (erg s^{-1} cm^{-3} Hz^{-1} ster^{-1}) and χ_ν is the extinction coefficient (cm^{-1}) $= \kappa_\nu \times \rho$. Here ds denotes the so called absolute derivative, along a geodesic ray in spacetime. In general

$$\frac{dI_\nu}{ds} = \frac{\partial I_\nu}{\partial t}\frac{\partial t}{\partial s} + \sum_{i=1}^{3}\frac{\partial I_\nu}{\partial x_i}\frac{\partial x_i}{\partial s} + \sum_{i=1}^{2}\frac{\partial I_\nu}{\partial \theta_i}\frac{\partial \theta_i}{\partial s} + \frac{\partial I_\nu}{\partial \nu}\frac{\partial \nu}{\partial s} \tag{45}$$

Which of these 7 components we retain depend on the complexity of the problem.

Photons travel with speed c, so $dt/ds = 1/c$. In a 1D, plane-parallel, non-moving case (choose z as axis name), we have

$$\frac{\partial I_\nu}{\partial x} = 0 \tag{46}$$

$$\frac{\partial I_\nu}{\partial y} = 0 \tag{47}$$

$$\frac{dz}{ds} = \cos(\theta) \tag{48}$$

$$\frac{d\theta}{ds} = 0 \tag{49}$$

$$\frac{\partial I_\nu}{\partial \phi} = 0 \tag{50}$$

$$\frac{\partial I_\nu}{\partial \nu} = 0 \tag{51}$$

$$\tag{52}$$

So we get (denoting $\mu = \cos(\theta)$)

$$\left[\frac{1}{c}\frac{\partial}{\partial t} + \mu\frac{\partial}{\partial z}\right] I_\nu(z,\theta,t) = \eta_\nu(z,\theta,t) - \chi_\nu I_\nu(z,\theta,t) \quad \text{Plane parallel, non-moving medium} \tag{53}$$

In spherical symmetry, the equation can be derived to be

$$\left[\frac{1}{c}\frac{\partial}{\partial t} + \mu\frac{\partial}{\partial r} + \frac{1-\mu^2}{r}\frac{\partial}{\partial \mu}\right] I_\nu(r,\theta,t) = \eta_\nu(r,\theta,t) - \chi_\nu I_\nu(r,\theta,t) \quad \text{Spher. symmetric, non-moving medium} \tag{54}$$

If we write $d\tau_\nu = -\chi_\nu \mu ds$, the plane-parallel case can also be written

$$\left[\frac{1}{c\chi_\nu}\frac{\partial}{\partial t} + \mu\frac{\partial}{\partial \tau_\nu}\right] I_\nu(r,\theta,t) = I_\nu(r,\theta,t) - S_\nu(r,\theta,t) \tag{55}$$

where S_ν is the source function

$$S_\nu = \frac{\eta_\nu}{\chi_\nu} \quad (\text{erg s}^{-1}\text{cm}^{-2}\text{Hz}^{-1}\text{Ster}^{-1}) \tag{56}$$

In general, η_ν and χ_ν depend in I_ν itself (through the influence of the radiation field on gas state as well as scattering emissivity), which means the transfer problem is "harder than it looks".

Formal solution (plane parallel, time-independent case)

By formal solution, we mean a solution for when η_ν and χ_ν (or equivalently S_ν) are explicitly, numerically known. Ignore for now the time-derivative term. Then we want to solve

$$\mu \frac{\partial I_\nu}{\partial \tau_\nu} = I_\nu - S_\nu \tag{57}$$

Or

$$\frac{\partial}{\partial \tau_\nu}\left[I_\nu e^{-\tau_\nu/\mu}\right] = -\frac{S_\nu e^{-\tau_\nu/\mu}}{\mu} \tag{58}$$

Then

$$\boxed{I_\nu(\tau_\nu) = \int S_\nu(\tau'_\nu) e^{-(\tau'_\nu - \tau_\nu)/\mu} \frac{d\tau'_\nu}{\mu}} \tag{59}$$

We will use this result to derive the solution in the diffusion limit.

Diffusion limit

In LTE (Local Thermodynamic Equilibrium), one can show that $S_\nu = B_\nu$ (the Planck function). Make a Taylor expansion around some point τ_0:

$$S_\nu(\tau) = B_\nu(\tau_0) + \frac{\partial B_\nu}{\partial \tau_\nu}|_{\tau_0} (\tau - \tau_0) + ... \tag{60}$$

Then

$$I_\nu = \int_{\tau_\nu}^{\infty} S_\nu e^{-(\tau'_\nu - \tau_\nu)/\mu} \frac{d\tau'_\nu}{\mu} \tag{61}$$

$$= [\tau'_\nu - \tau_\nu = x] = \int_0^\infty S_\nu e^{-x/\mu} \frac{dx}{\mu} \tag{62}$$

$$= B_\nu + \frac{\partial B_\nu}{\partial \tau_\nu}|_{\tau_0} \mu + ... \tag{63}$$

At high optical depth (deep in the "diffusion zone"), one can show that only first two terms are needed. The first moment (flux) becomes

$$\begin{aligned} F_\nu &= 2\pi \int_{-1}^{1} I_\nu \mu d\mu \\ &= 2\pi \left[B_\nu \int_{-1}^{1} \mu d\mu + \frac{\partial B_\nu}{\partial \tau_\nu}|_{\tau_0} \int \mu^2 d\mu \right] = \frac{4\pi}{3} \frac{\partial B_\nu}{\partial \tau_\nu}|_{\tau_0} \end{aligned} \tag{64}$$

We can write this

$$F_\nu = \frac{4\pi}{3}\frac{\partial B_\nu}{\partial T}\frac{\partial T}{\partial \tau_\nu}|_{\tau_0} = -\frac{4\pi}{3\chi_\nu}\frac{\partial B_\nu}{\partial T}\frac{dT}{dz} \tag{65}$$

The bolometric flux is

$$F = -\frac{4\pi}{3}\frac{dT}{dz}\int_0^\infty \frac{1}{\chi_\nu}\frac{\partial B_\nu}{\partial T}d\nu \tag{66}$$

Define the Rosseland mean absorption coefficient by

$$\boxed{\chi_R^{-1} = \int_0^\infty \frac{1}{\chi_\nu}\frac{\partial B_\nu}{\partial T}d\nu / \int_0^\infty \frac{\partial B_\nu}{\partial T}d\nu} \tag{67}$$

Then

$$\boxed{F = -\frac{4\pi}{3\chi_R}\frac{dB}{dT}\frac{dT}{dz} = -\frac{4\pi}{3\chi_R}\frac{dB}{dz}} \tag{68}$$

The use of the Rosseland coefficient give the exact right bolometric flux in a "gray" treatment. The Rosseland opacity, in LTE, depends on composition and temperature/density. We have obtained a conduction equation, where the flux of something is proportional to a gradient ($F = -K\nabla T$). The conductivity is in our case, using $B = (c/4\pi)aT^4$,

$$K_R = \frac{4c}{3\chi_R}aT^3 \tag{69}$$

Now we can see what to do with the energy transport term $\partial L(m,t)/\partial m$ in the 1st law of TD.

$$\frac{\delta e_{int}(m,t)}{\delta t} = s(m,t) - \frac{\partial L(m,t)}{\partial m} - p(m,t)\frac{\partial 1/\rho(m,t)}{\partial t} \tag{70}$$

Using also $dm = 4\pi r^2\rho dr$ so $d/dr = 4\pi r^2\rho d/dm$, and assume equlibrum so $e_{int} = aT^4/\rho$:

$$\frac{\partial L}{\partial m} = \frac{\partial}{\partial m}\left(4\pi r^2\frac{4\pi}{3\chi_R}\frac{dB}{dz}\right) \tag{71}$$

$$= \frac{\partial}{\partial m}\left(4\pi r^2\frac{16\pi^2 r^2\rho}{3\chi_R}\frac{\frac{c}{4\pi}aT^4}{dm}\right) \tag{72}$$

$$= \frac{16\pi^2 c}{3}\frac{\partial}{\partial m}\left(\frac{r^4}{\kappa_R}\frac{daT^4}{dm}\right) \tag{73}$$

This equation says that the net transport of internal energy is proportional to the gradient in flow, which in turn is proportional to the gradient in energy density. We therefore get a second derivative with respect to energy density for diffusive transport. This is the general property of any heat equation

$$\frac{\partial \phi}{\partial t} = \nabla \cdot [D \times \nabla \phi] \tag{74}$$

We now also know how to compute the emergent luminosity of the SN:

$$L_{surf} = 4\pi r_{surf}^2 \frac{4\pi c}{3\kappa_R} \frac{da T_{surf}^4}{dm} \tag{75}$$

A scattering LTE gas

The diffusion limit of the 1st law of thermodynamics (with Rosseland opacity) helps us to model the internal temperature evolution and the emergent bolometric luminosity to "medium" accuracy, not having to restrict ourselves to the adiabatic limit. The problem reduces to a single PDE in the variable T (plus specified ρ). We can also estimate the spectrum as a blackbody with the temperature at the photosphere location. Going further, and solving the transfer equation considering more detailed physics in the outer layers, we can achieve the goals

- Determine predictions for $L_{bol}(t)$ to high accuracy.
- Determine spectra.

The scattering atmosphere

The scattering atmosphere is a simplified model where radiation is emitted from an inner boundary - the photosphere - and then scatters (by electron scattering and line resonance scattering) in the outer layers.

The number of photons that Thomson scatter, per unit volume, time, and frequency is

$$N_\nu(\mu) = \sigma_T n_e \int_{-1}^{1} I_\nu(\mu') g(\mu', \mu) d\mu' \tag{76}$$

where g is the redistribution kernel, which in principle can depend also on frequency. For electron scattering it is

$$g = \frac{3}{4}\left(1 + \cos\left(\theta' - \theta\right)^2\right) \tag{77}$$

If we ignore this angle dependency, we get

$$N_\nu = \sigma_T n_e 4\pi J_\nu \tag{78}$$

The photons are reemitted, which is bookkept in the emissivity term:

$$\eta_\nu = \frac{N_\nu}{4\pi} = \sigma_T n_e J_\nu \tag{79}$$

Then $S_\nu = \eta_\nu / \chi_\nu = J_\nu$. The transfer equation then becomes

$$\boxed{\mu \frac{\partial I_\nu}{\partial \tau_\nu} = I_\nu - J_\nu \quad \text{Pure scattering}} \tag{80}$$

Integrate this equation over angle. Then

$$\frac{\partial F_\nu}{\partial \tau_\nu} = 0 \tag{81}$$

which tells us that (net) flux is constant with radius : we have no sources or sinks of energy in the atmosphere. (In non-planar case this becomes L = constant). First moment of the transfer equation:

$$\frac{\partial p_\nu}{\partial \tau_\nu} = F_\nu - 0 \tag{82}$$

As F_ν is constant,

$$p_\nu = F_\nu \tau_\nu + C \tag{83}$$

Gray case. For gray scattering $\tau_\nu = \tau$. Integrate over frequency:

$$p = F\tau + C \tag{84}$$

In equilibrium $p = 1/3aT^4$. We then get the result that

$$\boxed{T \propto (\tau + C)^{1/4} \qquad \text{gray opacity}} \tag{85}$$

In the so called Eddington approximation (not derived here), one can show $C = 2/3$, so $T = 0.93T_{phot}\,(\tau + 2/3)^{1/4}$, if we take the photosphere to be at $\tau = 2/3$. For a specified density profile and opacity, we then know the temperature profile of the atmosphere; it falls from T_{phot} at the photosphere to $0.84T_{phot}$ at the outer boundary ($\tau = 0$). In simple one-temperature models one therefore often takes $T = 0.9T_{phot}$ as an average value.

Numeric approaches

Apart from the two simple cases analyzed above, and a few more, the transfer equation has to be solved numerically by discretizing the (partial) differential equations into difference sums. This gives a set of coupled algebraic equations, which are solved by matrix inversion methods on the computer. E.g., let m denote spatial grid point and n angular grid point

$$\mu \frac{\partial I_{z,\mu}}{\partial z} = I_{z,\mu} - S_{z,\mu} \rightarrow \mu_n \frac{I_{m+1,n} - I_{m,n}}{z_{m+1} - z_m} = I_{m,n} - S_{m,n} \tag{86}$$

In general there are too many equations to solve simultaneously, so one implements some kind of iteration. Note that a problem with 100 radial cells, 100 frequencies, and 100 angles make 1 million equations, and 10^{12} matrix entries! Far beyond any computers capability, without iteration that breaks down the system into smaller chunks.

Overall picture : modelling the SN

Putting all components together, a model for the SN emergent radiation requires, for each zone:

- One equation involving the internal energy (some flavor of the 1st law of TD), which always has a T dependency.
- One equation for (radiative) energy transport, for each frequency and angle
  - Diffusion limit solution
  - Optically thin limit
  - RT equation
- One equation for each material electronic state modelled
  - LTE : Saha/Boltzmann equation $n_i = f(T, \rho)$.
  - Non-LTE : A rate equation depending on J_ν, T, other n_i.
- A (constitutive) relation specifying how κ_λ depend on populations (n_i) and T, for each frequency

Note that normally we do not have to compute the hydrodynamic evolution, as the SN reaches homology soon after explosion.

Expansion effects

We will now consider in more detail how lines contribute to opacity, and form spectral features that we can use to diagnose the *composition* of the supernova. Material from an explosion, like the galaxies in the Universe (from Big Bang) or the layers in a supernova, move at different velocities. The frequency of a light beam is different in each layer due to the Doppler shift:

$$\nu' = \nu \left(1 - \frac{v_{proj}}{c}\right) \tag{87}$$

where v_{proj} is the projected velocity along the direction of the beam. In supernovae $v/c \sim 0.01 - 0.1$. This is much larger than thermal line widths: $v_{th}/c \sim 10^{-5}$. This means that

A A photon Doppler shifts through a whole line profile over a small part of the ejecta ("it interacts locally").

B A photon can come into resonance with multiple lines, at different points, if their rest wavelength separation is $< v/c$.

A) Local line interaction (The "Sobolev limit"). The limit $v \gg v_{th}$ is called the Sobolev or high-velocity gradient limit. The photon will 'traverse' the line profile over a length $L_{Sob} = v_{th}/(dV/dr)$, where dV/dr is the velocity gradient. As $V = r/t$ in homology, $dV/dr = 1/t$ and $L_{Sob} = v_{th}t$. As $v_{th} \ll v$ this region is small compared to the size of the SN. For a top-hat line profile ($\phi = 1/\Delta\lambda_{th}$):

$$\boxed{\tau_{Sob} = \sigma n_l L_{Sob} = \frac{h\lambda_0}{4\pi} B \frac{1}{\Delta\lambda_{th}} \times n_l \times \frac{\Delta\lambda_{th}}{\lambda_0} ct = \frac{hc}{4\pi} B n_l t} \tag{88}$$

One can show that this holds for *any* line profile. The optical depth depends only on the local number density (n_l) at the point of resonance. Ignoring changes in ionization/excitation, $n_l \propto t^{-3}$, so $\boxed{\tau_{Sob} \propto t^{-2}}$.

B) Expansion opacity. If there is a typical velocity separation ΔV_{sep} between optically thick lines around wavelength λ, the mean-free path is[1] $x = \Delta V_{sep} t$. Write $\Delta V_{sep} = c\Delta\lambda_{sep}/\lambda$. Then, since $\kappa = 1/(x\rho)$,

$$\boxed{\kappa_\lambda^{line,exp} \approx \frac{\lambda}{ct\rho\Delta\lambda_{sep}}} \tag{89}$$

Now say there is only probability $1 - \exp\left(-\tau_{Sob}^i\right)$ that line i interacts. Then refine the formula as

$$\boxed{\kappa_\lambda^{line,exp} \approx \frac{1}{ct\rho} \frac{1}{N} \sum_{i=1}^{N} \frac{\lambda_i}{\Delta\lambda_i} \left(1 - e^{-\tau_{Sob}^i}\right)} \tag{90}$$

where the set of N lines have be chosen over some wavelength range centred on λ.

This is called an expansion opacity. Figure 5 shows an illustration. Note that this is not an exact opacity like the other ones- this is because line interaction is not a continuous process but occurs at discrete points in the Sobolev limit. As opacity can only defined as some integral average for lines, there is always some degree of arbitrariness how this is done (as the photon paths cannot be defined a priori). Line opacity is together with Thomson opacity typically the most important in SNe. In KNe it is completely dominant.

Photospheric ("P Cygni") line formation

Consider now a moving scattering atmosphere in the Sobolev limit. We will study what line profile arises from a single optically thick line, with the parameters $h = V_{phot}/V_{max}$, and ϵ (the "destruction probability") (1-ϵ for scattering).

Divide the SN into "sheets" perpendicular to the line of sight. The projected velocity in each sheet is a constant $V_{proj} = V\cos\alpha = V\frac{V_z}{V} = V_z$. Thus,

[1] This is often denoted λ, but we use x here to avoid confusion with the wavelength

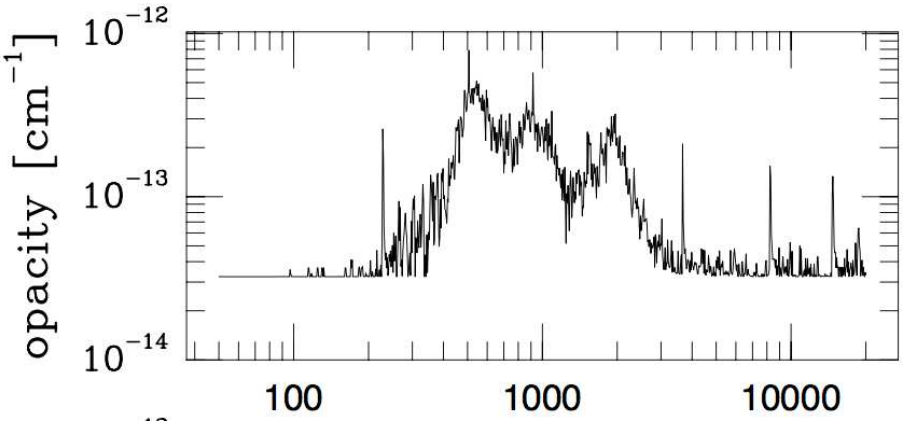

Figure 5: Expansion absorption coeffient (called opacity in the paper from which plot was taken) for solar composition gas in LTE at $T = 15,000$ K, $\rho = 10^{-13}$g and $t = 15d$. From Blinnikov 1998 (using Eq. 90). The x-axis is wavelength in Å. The Thomson contribution is the "floor" value at 3e-14. In the UV (between 500-3000 Å), the line expansion opacity is a factor several times larger than the electron scattering one.

each sheet gives line resonance at a Doppler shifted wavelength $-\lambda_0 V_z/c$ in the observer frame ("blueshift for approaching side"). When absorbing, the sheet hinders flux at this wavelength to reach the observer.

Consider Fig 6. We delineate two cases.

- **Case I**. $h > 0.71$: Full photosphere is never blocked by a sheet $\rightarrow$ only partial absorption.
- **Case II**. $h < 0.71$. Photosphere is fully blocked by sheets in B region $\rightarrow$ complete absorption.

The ABC regions behave as following:

- **A**: Whole resonance sheet covers photosphere. Area of sheet grows going inwards, giving deeper absorption.
- **B-Case I**: Whole resonance sheet covers part of photosphere. Sheet area is constant (derive!), giving flat bottom in profile. Absorption depth is $(1 - h^2)/h^2$ (derive!)
- **B-Case II**: (Part of) resonance sheet covers whole photosphere. Also flat bottom, but at complete absorption.
- **C**. A declining fraction of photosphere is blocked, giving declining absorption.

Figure 5 shows resulting line profiles for Case I. We see that

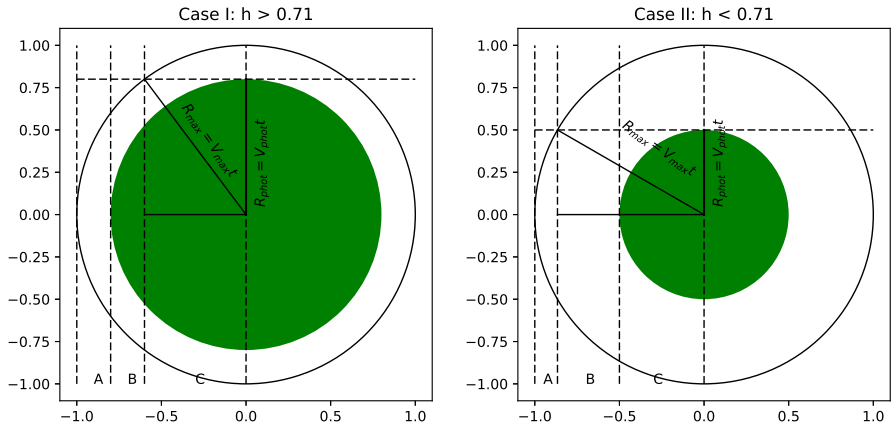

Figure 6: Geometry of P-Cygni line formation.

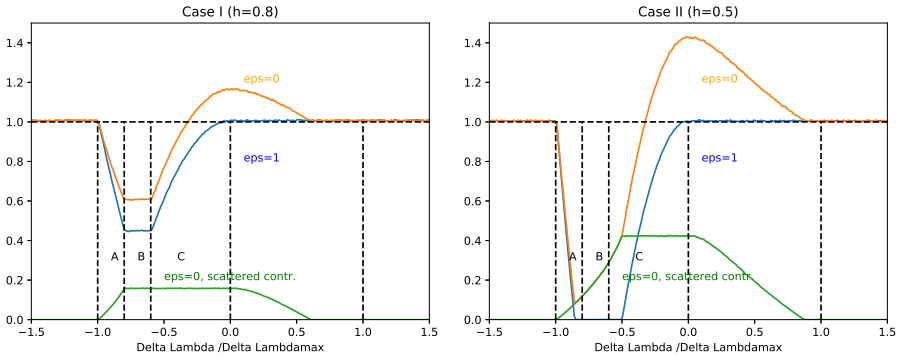

Figure 7: Line formation for Case I (left) and Case II (right).

- **Destructive line** ($\epsilon = \mathbf{1}$). Absorption starts at $-V_{max}$, reaches min at $-V_{phot}$, is flat (partial absorption) to $\sqrt{1-h^2}$, and then moves back towards zero.
- **Scattering line** ($\epsilon = \mathbf{0}$). Reemission adds the green distribution. The location of minimum does not change. For redshifted photons from the receding side of the SN, some scattered photons are "blocked" by photosphere. The peak is at zero shift.

For such lines, we can clearly determine both V_{max} and V_{phot}. In addition, ϵ can be determined from the height at $x = 0$. V_{max} can be linked to a density $n(V_{max})$ by modelling. For Case II, Vphot is uniquely determined by the minimum. These kind of line profiles are called "P-Cygni like" after their initial observations in LBV star "P-Cygni" showing rapid outflow speeds.

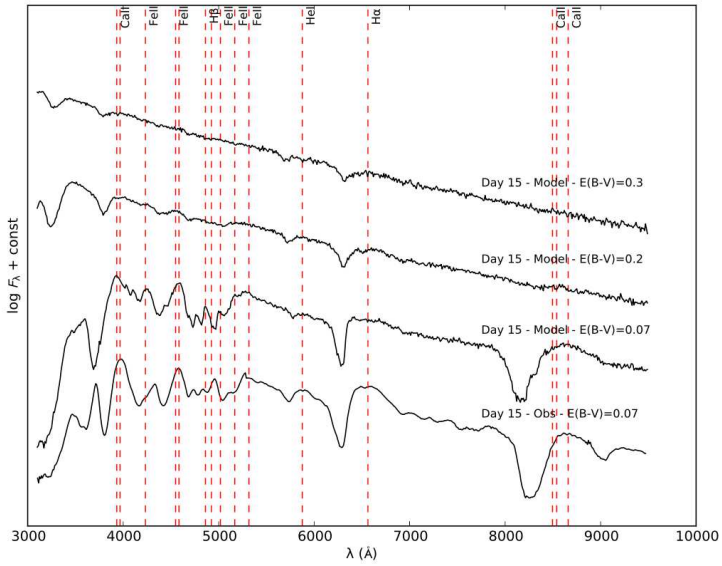

Figure 8: An observed Type IIb SN spectrum showing P-Cygni lines (bottom curve).

Nebular phase line formation

At later times, the photosphere disappears and we enter the nebular phase. Now, the spectrum consists of emission lines. As powering comes from radioactivity, mainly emission from the inner region where ^{56}Ni resides. Figure 9 shows line profiles in 6 cases, of which we comment on 3:

- **Uniform sphere**. For uniform conditions, each sheet now contributes flux at wavelength $-\lambda_0 V_z/c$ in proportion to its area $A = \pi p^2 = \pi(R_{out}^2 - R_z^2) \propto 1 - (\Delta\lambda/\Delta\lambda_{max})^2$. Line profile is a parabola.
- **Thin shell**. $A = \pi((p+\Delta p)^2 - y^2) \approx 2\pi p \Delta p$. Because $p = \sqrt{r^2 - z^2}$, $\Delta p/\Delta r = 1/2\left(r^2 - z^2\right)^{-1/2} 2r = r/p$, $p\Delta p = r\Delta r = constant$.The line profile becomes a flat top.
- **Gaussian**. One can show that also line profile becomes a Gaussian (see "Handbook of SNe chapter" for details).

Figure 10 shows an example of an observed nebular spectrum.

The frequency-integrated emissivity in a line is, in the Sobolev approximation

$$j = \frac{1}{4\pi} n_u h\nu A \beta_{Sob} \quad \text{erg/s/cm3} \tag{91}$$

where $\beta_{Sob} = (1 - e^{-\tau_{Sob}})/\tau$ is the Sobolev escape probability. Consider two limits

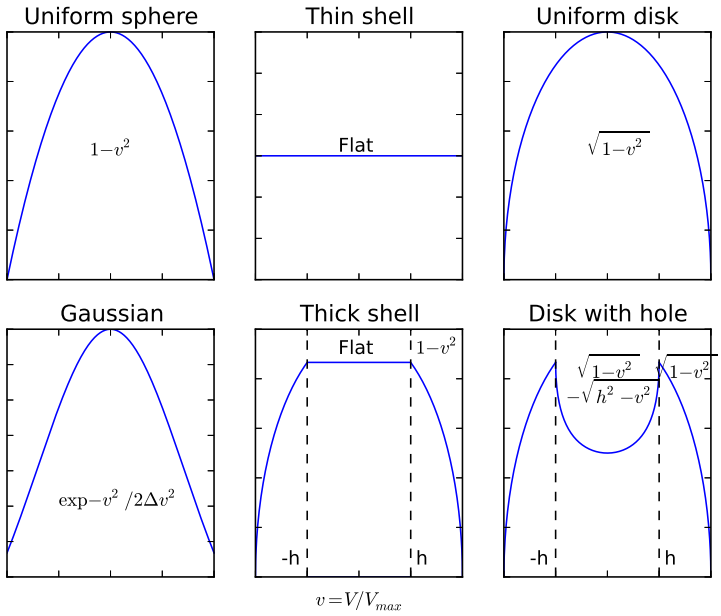

Figure 9: Nebular line profiles for 6 different cases. From Jerkstrand 2017 (Handbook of SNe).

- **Optically thin line** ($\beta_{Sob} \rightarrow 1$). Then total luminisity depends on $jV \propto N_u$, i.e. one can get mass of ion.
- **Optically thick line**($\beta_{Sob} \rightarrow 1/\tau_{Sob}$). Then total luminosity depends on $Vn_u/n_l = V \times f(T)$. Can get volume of emitting region.

Overview of observed classes, main results, open questions

Table 4 shows an overview of the main SN classes, their fraction of all SN per volume of space, the stars believed the be the sources of them, typical estimated values for E, M, R_0, $M(^{56}\mathrm{Ni})$ inferred from modelling, and composition that has been diagnosed. A few comment on current ideas are given below.

Type II SNe

The hallmark of Type II SNe is H in the spectra. On a more detailed level this class subdivides into three: IIP, IIL and IIn. This is a somewhat awkward classification as "P" and "L" refer to light curve shape ("Plateau" and "Linear (decline)"), but "n" refers to a spectral property ("narrow lines"). The IIP class is much more common than the other two. It is the only SN class for which we

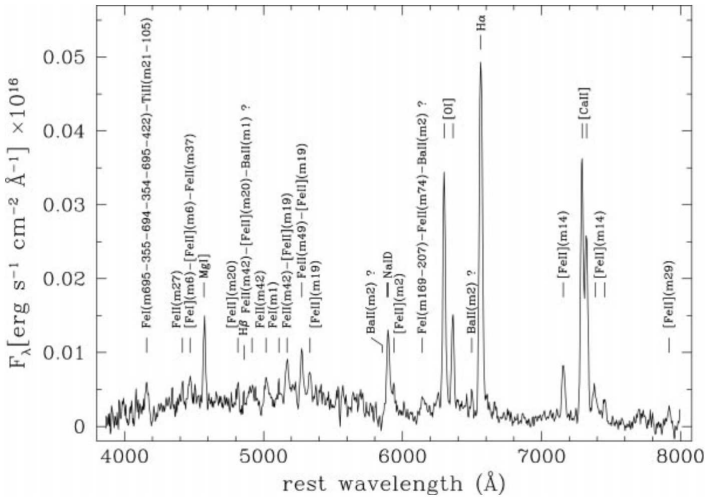

Figure 10: Example of an observed nebular spectrum from a narrow-lined Type IIP SN. From Benetti et al. 2001. These narrow-lined Type IIP SNe have inferred energies of 10^{50}erg, and are hypothesized to come from the lowest mass stars in the 8-12 $M_\odot$ range.

Type	Fr.	Origin	R_0	M_{ej}	E_{kin}	M(^{56}Ni)	diag. comp.
II	50%	RSGs	100-1000	5-30	10^{50-51}	0.01-0.1	C,O,Na,Mg,Ne,Si,S,Ar,Fe,Ni
Ibc	25%	He star	$\lesssim 10$	1-5	10^{51-52}	0.05-0.2	C,N,O,Na,Mg,Ca,Si,S,Fe,Ni
Ia	25%	WDs	<0.1	~ 1.4	$\sim 10^{51}$	∼0.5	Ca,Si,S,Fe,Co,Ni
SLSN	0.01%	VMS	?	5-50	10^{51-52}	?	O,Mg,Ca,Fe*
KN	∼0.1%	NS	<0.1	0.01	10^{51}	–	r-process

Table 4: Overview of SNe and their inferred properties.

have direct progenitor confirmation (RSGs) from archival images. A RSG origin is also robustly inferred from the LC shape, which from simple considerations requires R_0 of several hundred, as realized already in the 1970s.

The study of IIP SNe is therefore at the stage where we try to determine some rather detailed properties of these RSGs, their nucleosynthesis, and explosion dynamics. As perhaps hinted by our finding of quite weak dependencies of fundamental observational properties on E, M etc, there is quite some disagreement between different models and methods. For example, some methods indicate that stars in the 20-30 $M_\odot$ range explode as IIP SNe, whereas other methods indicate they do not. Figure 11 shows an example of such a model fit to a light curve and Fig 12 to photospheric spectra. By their sheer number, IIP SNe give perhaps the best hope still to establish relations between properties such as progenitor mass and explosion energy.

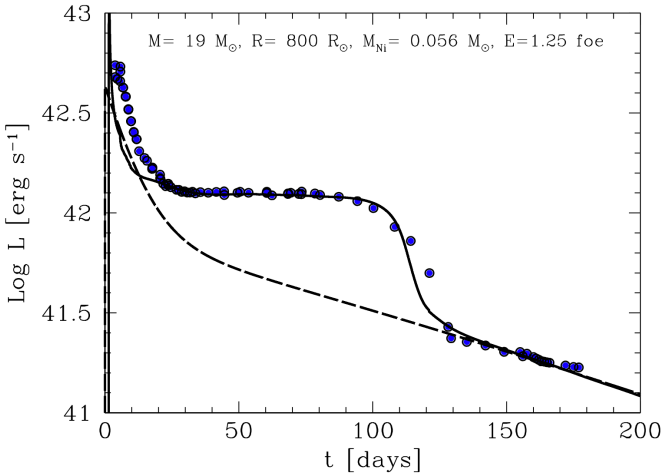

Figure 11: Example of a Type IIP model fit (black, solid) to an observed SN (blue dots). From Bersten et al. 2011. Values for the 4 fit parameters are written at top. From Bersten et al. 2011.

Type Ibc SNe

Type Ibc SNe have no H, so the envelopes of these progenitor stars must have been lost somehow[2] There are two main mechanisms for this; a wind-driven mass loss (radiation pressure continously blows outer layer away), or gravitational overflow to a binary companion. A key diagnostic of this should be the ejecta mass; wind-driven mass loss is predicted to occur only for quite massive stars ($M_{ZAMS} \gtrsim 30$) that should have large ejecta masses ($M_{ej} \gtrsim 5$). However, already 30 years ago did consideration of Δt (which is of order 30d) indicate that M was only a few solar masses (see also Fig. 13 for a recent example). This seems more consistent with an origin in lower-mass stars. Evidence from line studies point in the same direction (Fig. 14).

Another active research area is to understand what truly distinguishes Ib (show He lines) and Ic SNe (do not show He lines). While it was initially assumed that the lack of He in Ic SNe meant they had lost also their He layers, later work has highlighted that He is not so easy to excite and is perhaps just "invisible" sometimes depending on ejecta conditions. This question has not yet been settled. Roche lobe overflow of also the He layer is much harder to achieve than the H layer (the star shrinks when all H is lost), so if Ic SNe are truly He free this is not easy to explain in the binary scenario. For wind mass loss, even higher masses are needed to strip away also the He, but such masses are not indicated from their LC widths, which are similar to those of Ib SNe. The origin of Ic SNe remains a mystery.

[2]Here, we count also the "IIb" class. Although IIbs have some small amounts of H, they have lost virtually all their H envelopes.

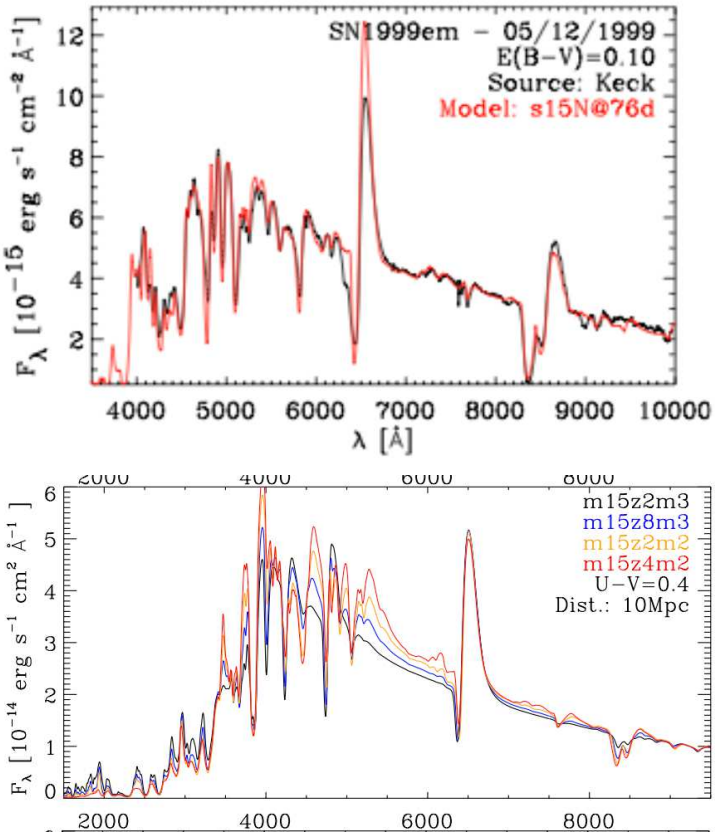

Figure 12: *Top*: Example of a Type IIP photospheric phase spectral model (red) compared to an observed spectrum (black) at 75d post explosion. *Bottom*: Spectral dependence on envelope composition (metallicity). From Dessart et al. 2013.

A particular class, the *broad-lined Ic SNe*, seem to involve unusually high energies and at least sometimes have high inferred masses, indicating a true massive star origin. Some of them have associated *Gamma-ray Bursts*, and perhaps explode by a fundamentally different (MRI) mechanism rather than the neutrino one.

Type Ia SNe

Type Ibc and Ia SNe have quite similar light curves, although Ias tend to be brighter. However, their spectra are quite different and in the mid 1980s it became established that these were two fundamentally different types of explosions. The higher brightness of Ias has two reasons: i) A higher ^{56}Ni mass ii) A lower ejecta mass, which gives a shorter diffusion time and peak at an earlier

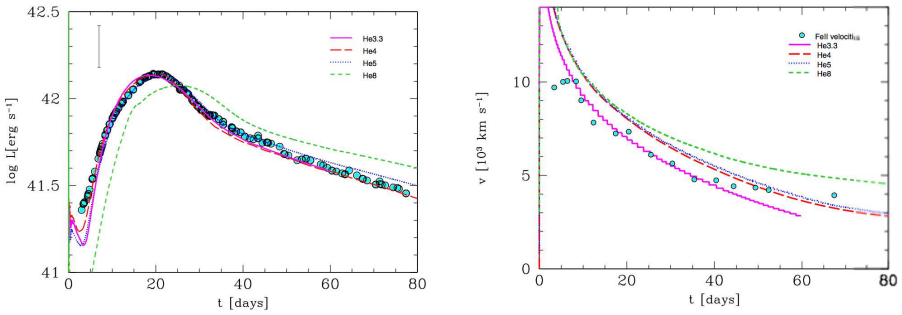

Figure 13: Example of a Type Ib model fit. Four different He cores (masses 3.3, 4, 5 and 8 $M_\odot$) were exploded with energies of 0.6,1,1.2, and 2 Bethe (10^{51} erg). The first three models fit the observed LC well, but the most massive one peaks too late. Note that as diffusion time is degenerate in M^3/E (Eq 9) one cannot uniquely constrain M and E without fitting also a velocity ($\propto \sqrt{E/M}$). the figure on the right shows that the He8 model already has too high photospheric velocities (using $E = 2$), and this model fit can therefore not be improved by increasing E (which could otherwise move the peak earlier). From Bersten 2012.

time when the radioactive input is higher (Arnett law).

Today we know these are from white dwarfs that initiate collapse as the mass becomes too high (above the Chandrasekhar limit) by some accretion or merger process. By very early observations it has recently been demonstrated that the progenitor is indeed very small, much smaller than a normal star.

As with Type IIP SNe, with the progenitors reasonably well known, current research tries to constrain some detailed properties. The "holy grail" is to determine whether these are single WDs that accrete matter from a normal star, or whether its two white dwarfs merging by gravitational wave radiation (or both). Figure 15 shows one estimate of the distribution of masses for Ia SNe, which can put constraints on their origin.

Superluminous supernovae (SLSN)

SLSNe were discovered around 2005: very rare SNe about 100 times brighter than normal. They come in two spectroscopic classes: IIn and Ic. The IIn class ("n" for narrow lines) probably derives its luminosity from collisions with unusually large amounts of circumstellar material at relatively large radii. As $E_{rad,tot} \sim 10^{51}\text{erg} = E_{kin}$, one needs efficient conversion and $M_{CSM} \gtrsim M_{SN}$. Where such large amounts of CSM would come from is unclear. Giant eruptions are known for some H-rich stars such as LBV, but there is no known mechanism to synchronize an eruption and core collapse (which typically need to occur within a few years of each other).

The Ic class shows no sign of interaction: these SNe seem powered by either very large amounts of ^{56}Ni or energy from the central pulsar or black hole. As

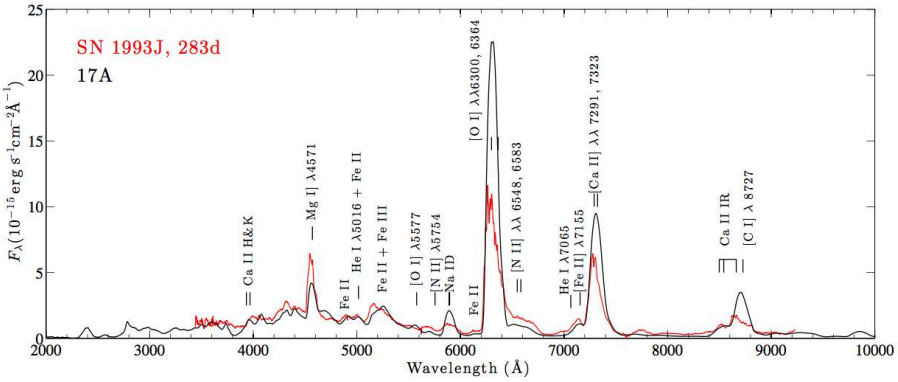

Figure 14: Nebular line model of a $M_{ZAMS} = 17\ M_\odot$ star (black) for a Type IIb SN (red). The model overproduces lines from O, Ca, and C, which indicates that the observed SN has less nucleosynthesis and comes from a somewhat lower mass progenitor. Note also the asymmetry of observed line profiles compared to the symmetric (1D) model. This means the ejecta have clear 3D structure. From Jerkstrand et al. 2015.

we saw earlier, the ^{56}Ni hypothesis has great difficulty to provide enough power without increasing the ejecta mass too much - at least for some of these (the fast evolving ones). It has therefore been proposed that the powering comes from the central region. The energy reservoir in a rotating neutron star is $E = 10^{52} P_{ms}^{-2}$ erg, sufficient to release the observed 10^{51} erg of radiated energy if the efficiency factor is $\gtrsim 10\%$. The energy can be released by dipole spindown (which powers normal pulsars), which has a characteristic energy input time-scale of

$$\tau_{spin} = 5 \text{ days } P_{ms}^2 B_{14}^{-2} \tag{92}$$

Thus, is the neutron star is born spinning fast enough (1-10 ms) and has high enough magnetic field ($\sim 10^{14}$ G), this mechanism can work. However, many question marks remain and the mechanism needs to be demonstrated by detailed simulations, which is difficult. Another hypothesis is that the luminosity comes from residual accretion onto a newly formed black hole. Accretion can release up to 40% of rest mass energy for rotating black holes, which is only 10^{-3} solar masses to account for 10^{51} erg. However, also here specific calculations for the details are needed.

Recently, we obtained the first comprehensive view of the content of these exotic SNe by a series of nebular phase spectra (Fig 16). They show very high masses of oxygen, magnesium and silicon moving at very high velocities (SLSN Ic are in fact all broad-lined Ics). This points to the origin in very massive stars, and probably an explosion by a mechanism different than the neutrino one.

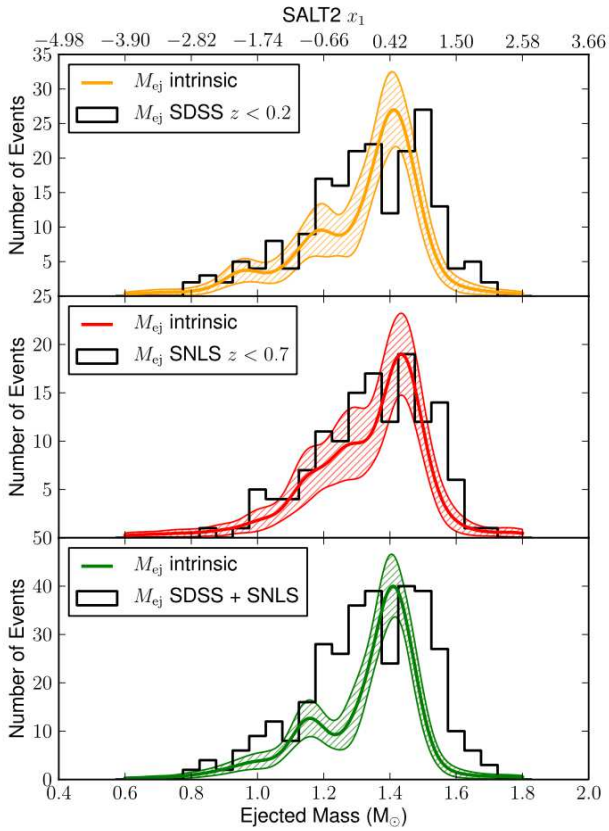

Figure 15: An estimates for Type Ia ejecta mass distribution. From Scalzo et al. 2014.

Study questions for exam

Lesson 1

- What is the first law of thermodynamics, and what terms does it contain?
- What is the internal energy for radiation-domainted gas in equilibrium?
- Derive what $pd/dt(1/\rho)$ becomes assuming homology and pressure dominated by radiation.
- Solve the 1st law of TD in the adiabatic limit. What time evolution do you get for e_{int} and T?
- Which parameters does the light curve duration depend on? Explain why increasing each parameter lengthens or shortens the LC. What is the caveat for Type IIP SNe?

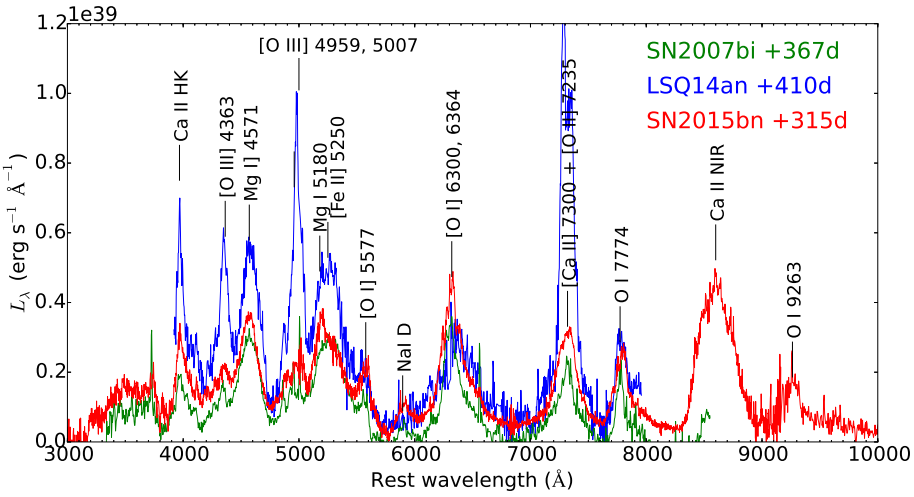

Figure 16: Nebular spectra of superluminous Ic SNe. From Jerkstrand et al. 2017.

- Which parameters does the brightness depend on, assuming only a) explosive energy release? b) radioactivity?
- What is Arnett's law?

Lesson 2 and 3

- Derive how $T_{phot}(t)$ depends on $L(t)$ and $V_{phot}(t)$. Discuss how it may vary over a light curve evolution.
- Derive parameters (E,M,κ) for the kilonova AT 2017gfo. ($t_{peak} = 1d$, $L_{peak} = 1E42$ erg, T_{phot}=8500 K.
- Name three types of photon-electron interactions, and describe their dependence on gas state and wavelength.
- For a given opacity, estimate how long the SN is optically thick.

Lesson 4

- Describe what is meant by *specific intensity*, *mean intensity*, *flux*, and *pressure*?
- What is the general transfer equation (what are names of terms and what do they mean) and what is d/ds? Derive the form of the transfer equation in a simple case.
- Derive a formal solution for a simple limiting case.

- How can solution to the transfer equation give us the dL/dm term in the 1st law of TD? What is the Rosseland absorption coefficient and why is it useful?
- Derive and discuss some properties of a purely scattering atmosphere. What are generic properties of F, p and T?

Lesson 5

- Describe how photons interact with lines in a rapidly expanding medium like a SN. What is the Sobolev approximation?
- Describe the basics of photospheric line formation. What parameters can an observed line tell us?
- Describe the basics of nebular line formation. What parameters can an observed line tell us?
- Review the main SN classes with regard to typical properties, current theories for their origin, and outstanding questions.